4-2022

Visible Light Illuminated Tin Oxide-Gold Nanoparticle Schottky Junctions for H2O2 Generation in Water

Sarah Glass

Visible Light Illuminated Tin Oxide-Gold Nanoparticle Schottky Junctions for H_2O_2 Generation in Water

by
Sarah Glass

Undergraduate honors thesis under the direction of
Dr. Kevin McPeak
Department of Chemical Engineering

Submitted to the LSU Roger Hadfield Ogden Honors College in partial fulfillment of the Upper Division Honors Program.

April, 2022

Louisiana State University
& Agricultural and Mechanical College
Baton Rouge, Louisiana

Table of Contents

List of Figures

Abstract

Solar disinfection of water using sunlight is an attractive solution to the global water crisis, however most of the systems that currently exist only use the ultraviolet (UV) portion of sunlight (~5% of the spectrum by energy). A system that uses the visible portion of sunlight (~40% of the spectrum by energy) has potential to be a more efficient disinfector.

SnO_2 is a wide-band gap semiconductor which exhibits a favorable conduction band alignment with Au for the generation of ROS (Reactive Oxygen Species). ROS has the power to disinfect water. SnO_2 does not absorb sunlight because it requires a higher excitation energy than what sunlight provides. Gold nanoparticles strongly absorb visible light through their plasmon resonances with an absorption spectrum that is highly tunable based on the size and shape of the particle and the local environment they are in. Recently, researchers have shown that plasmon resonances can decay into above-equilibrium "hot" carriers (e.g. electrons and holes) that can drive electrochemical reactions. One promising architecture for hot-carrier collection is hybrid metal-semiconductor junctions. Therefore, SnO_2 in conjunction with gold nanoparticles is a system that will use visible light (~400nm-700nm).

It can be proven that visible light is the driver of the reaction because when the wavelengths were limited to light>450nm the reaction proceeded at a rate similar to when all sunlight was used. This has prospective to efficiently drive electrochemical reactions by utilizing a more abundant portion of sunlight.

Chapter 1: Semiconductor/Metal Schottky Junctions for Usage of Reactive Oxygen Species Generation

1.1 Introduction

The use of plasmonic metal-semiconductor Schottky Junctions for the purpose of ROS generation is a plausible method of utilizing sunlight for means of water disinfection. Common methods of utilizing sunlight to generate hot carriers (electrons that are able to drive chemical reactions) use the Ultraviolet (UV) portion of the solar spectrum to drive reactions. While UV light is high energy, it only makes up a small portion of energy provided by the sun. Figure 1.1.1 shows the entire solar spectrum with accordance to color wavelength. Figure 1.1.2 is a solar flux diagram that can be integrated to show power at each light region. Using this method, the sun provides ~30 W/m^2 in the UV region and ~250 W/m^2 in the visible region. The sun provides roughly 8x more power in the visible light (400-600nm) region than UV (280-400nm) region, making visible light an attractive option for generating hot carriers.

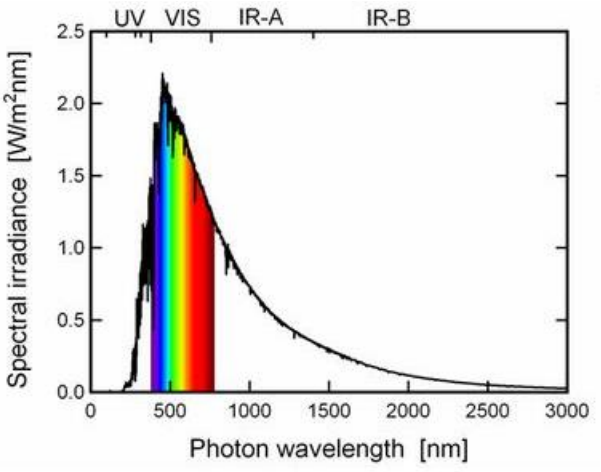

Figure 1.1.1. **Diagram of Solar Spectrum** Ultraviolet (UV) light ranges 280-400nm, visible light ranges from 400 to 700nm.

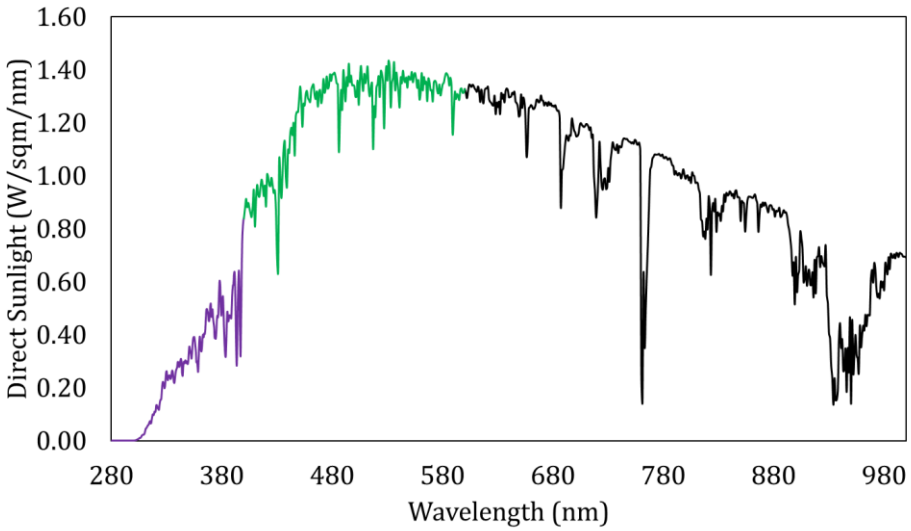

Figure 1.1.2. **Diagram of Solar Flux** UV is highlighted in purple, Visible (400-600nm) is highlighted in green, higher wavelengths are black. This flux can be integrated to give power of each light region.

1.2 Semiconductors for Reactive Oxygen Species Generation

Semiconductors are materials that lie between metals and insulators in that they have a small gap between the valence band and conduction band, illustrated in Figure 1.2.1. This allows energy, such as photons or light energy, to excite electrons from the valence band into the conduction band where they are able to drive chemical reactions.

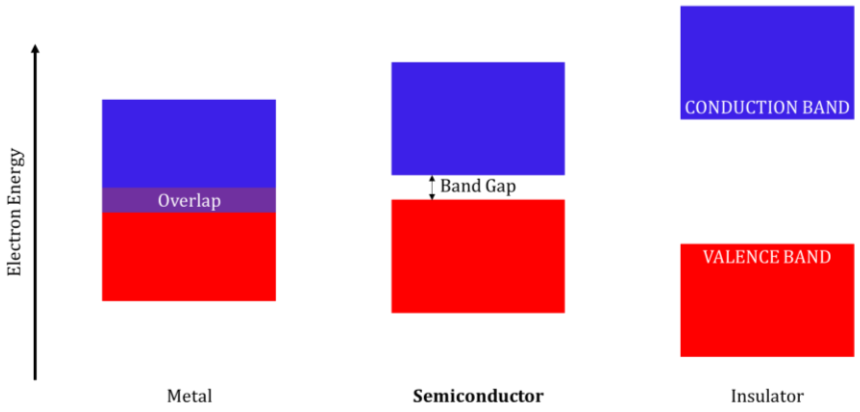

Figure 1.2.1. **Diagram of Semiconductor Materials** Semiconductors have a space between the valence band and the conduction band that allows electrons to move across when excited by energy. This gap is much larger in insulators and nonexistent in metals.

These chemical reactions that occurs include reduction and oxidation reactions that generate Reactive Oxygen Species (ROS). ROS is a category of highly reactive derivatives of elemental oxygen. These chemicals can be used to destroy or deactivate bacteria and viruses, thus becoming very useful in water disinfection. ROS has many generation pathways, shown in Figure 1.2.2.

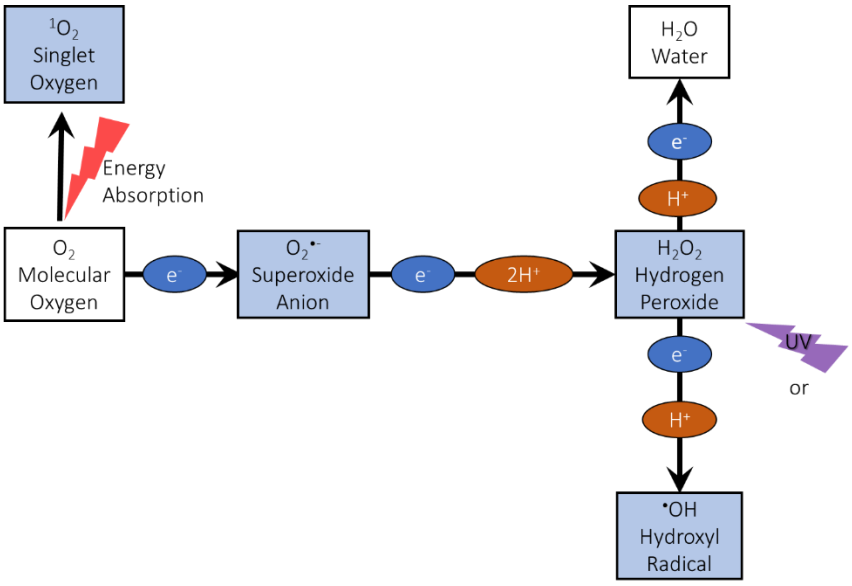

Figure 1.2.2. **Diagram of ROS Generation Pathways** This research is focused on Hydrogen Peroxide (H_2O_2) generation, so the main pathway is reduction of dissolved oxygen in water to form a super oxide anion ($O_2\bullet$). This chemical is then reacted to form H_2O_2. Further reaction of the H_2O_2 molecule can result in harsher ROS or water.

ROS generation using semiconductors can be done in many ways, the simplest of these being photoexcitation of a semiconductor with a band gap equivalent to UV light energy (3.2 eV). An example of this is TiO_2 and its mechanism for ROS generation is shown in Figure 1.2.3. Here photo excitation is used to generate electrons that can drive ROS generation reactions, and this is due to UV light having enough energy to excite the electron within TiO_2.

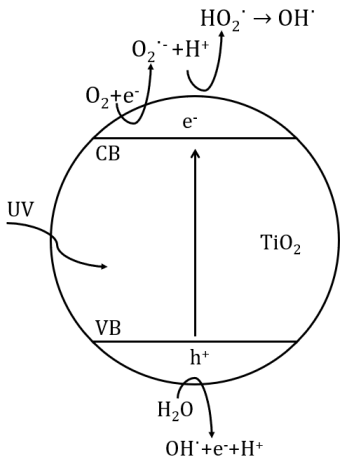

Figure 1.2.3. **Diagram of UV Illumination TiO_2 and Reactive Oxygen Species Generation Mechanism** When TiO_2 is illuminated with UV light, the electrons in the valence band are excited to the conduction band state, where the hot carrier are used to reduce dissolved oxygen in the surrounding water and the hot hole left behind is used to oxidize water, these reactive oxygen species are then left in the water.

The desire to use visible light stems from a more abundant power source, however this source does come at a lower energy. Semiconductors that have band gaps with widths equivalent to visible light exist (GaP, CdS, etc.), however, these semiconductors are often expensive, unstable, or toxic. For application of water disinfection, stability is of the utmost importance.

Use of UV light accepting semiconductors in conjunction with stable metals is another method for ROS generation, however UV light is still the source of energy. Shown in Figure 1.2.4, this system treats the metal as an electron scavenger.

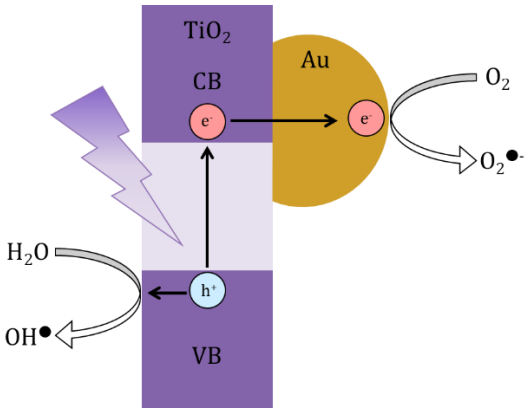

Figure 1.2.4. **Diagram of TiO_2 and Gold Metal System for ROS Generation** This system uses the UV excitation of TiO_2 to generate hot electrons, metals is used solely as an electron scavenger.

The use of UV light has proven to be an efficient way to generate ROS in water, however exploration of visible light in this application is important because it hold potential for photocatalytic ROS generation to be an effective and reliable method using only direct sunlight.

1.3 Semiconductor Metal Schottky Junctions

Wide band gap semiconductors can prove to be inactive under solar irradiance, in this case not absorbing any visible or UV light. This leave opportunity for a visible light absorber, such as a metal nanoparticle, to inject electrons into the inactive semiconductor to create an ROS generating Schottky Junction. In this research this system is modeled using Tin Oxide (SnO_2) and Gold Nanoparticles (AuNPs), and is shown in Figure 1.3.

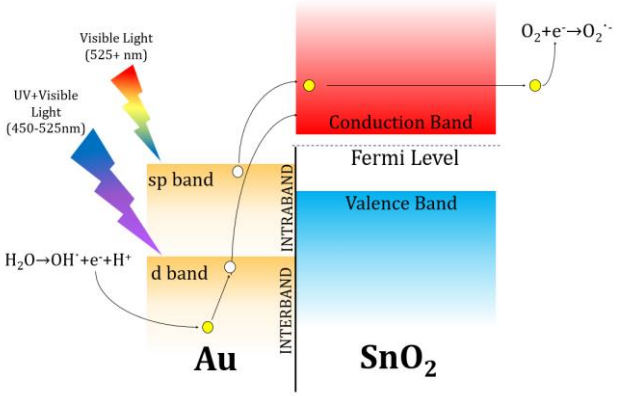

Figure 1.3. **Diagram of Visible Light Illumination of Tin Oxide and Gold Nanoparticle Schottky Junction and the Resulting Photocatalytic Reactive Oxygen Species Generation** When gold nanoparticles are excited by visible light the sp band electrons are excited and move into the conduction band of the tin oxide, overcoming the Schottky barrier. The hot carrier can then reduce dissolved oxygen from the surface of the Tin Oxide. The hot hole left behind can oxidize the water from the surface of the gold nanoparticle.

The band gap of SnO_2 is ~3.8 eV, which can be converted to ~326 nm. This is a wavelength outside of the sun's abundant radiation and leaves SnO_2 as a material that is not excited using solar energy. Gold however can be formed into nanoparticles that are tunable based on size and can be tuned to absorb visible light. Electrons in the SP band of the AuNP can be excited using visible light and injected into the conduction band of SnO_2, where they are able to reduce oxygen and complete the first step in generating H_2O_2.

1.4 Overview of Presented Research

This research aims to generate ROS under visible light excitation using hot carriers generated from a metal nanostructure. The aims of this research are to design and fabricate a reusable photocatalytic system, explore the effects of hole scavengers on H_2O_2 generation, and test the effects of oxygen concentration in SnO_2 films on the efficacy of producing H_2O_2.

Chapter 2: Fabrication and Analysis of SnO_2/AuNPs System for H_2O_2 Generation

2.1 Introduction

Each step in thin film preparation is extremely important and delicate. The films used in this system range from 2-200 nm, all on a scale that is not visible to the human eye. To produce each 1x1 inch sample, days of fabrication and many steps are taken to ensure correct properties.

These samples start with a glass backing, using Soda Lime Glass, or microscope slides, as a robust and cheap structure. Then an aluminum layer is deposited using metal evaporation under near vacuum conditions. This aluminum layer is over 100nm thick and deposited quickly to avoid any oxidation of the aluminum. A very thin, ~5nm, layer of chromium is used as an adhesion layer between the glass and aluminum, however this has no optical effects on the final sample. An SnO_2 layer, roughly 50nm thick, is then deposited using RF sputtering. Lastly, a thin gold film is deposited via evaporation and annealing to create gold nanoparticles on top of the SnO_2 film. Figure 2.1 shows a schematic of deposition order in the samples.

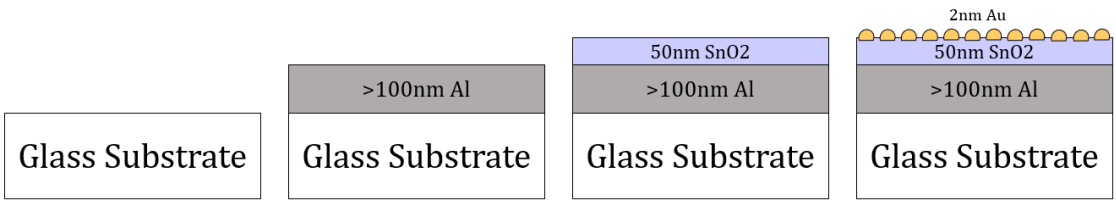

Figure 2.1. **Diagram of Experimental Samples Deposition Order** Glass substrates are cleaned, and a thin layer of Aluminum is deposited with an adhesion layer of Chromium. A thin film of tin oxide is then deposited using RF sputtering and annealed. Lastly, gold is evaporated onto the samples and annealed to form nanoparticles, using gold dewetting technique.

2.2 Materials and Methods

2.2.1 Tin Oxide Thin Film Preparation

The SnO_2 film is deposited via Radio Frequency (RF) sputtering. A ceramic SnO_2 target is used. 5% O_2/95% Argon gas is used with a working pressure of 3.4 mTorr. The thickness of the samples is a product of the distance from the target, 7.5cm, the power used to sputter, 25W, and the time the sample is exposed to the plasma, 3.5 minutes. These conditions are illustrated in Figure 2.2.1.1 and many rounds of trial and error were done to result in these conditions. All layer thickness testing was done using a profilometer.

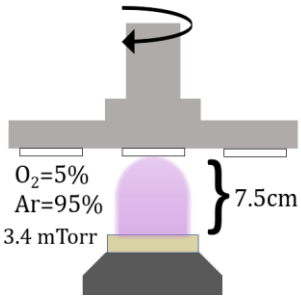

Figure 2.2.1.1. **Diagram of Sputtering Technique used to Deposit Tin Oxide Thin Film** Ideal Tin Oxide thin films of 50nm were created using a target-sample distance of 7.5cm and a working pressure of 3.4 mTorr. Samples generated for initial H_2O_2 generation tests were generated using 5/95 volume% Oxygen/Argon content.

Once samples are sputtered, they are annealed at 400C for 1 hour. This improves the crystallinity of the SnO_2 films greatly. X-Ray Diffraction (XRD) testing is shown in Figure 2.2.1.2. This quantifies the film is SnO_2 based on the Bragg peaks present at the miller indices of 110, 101, and 211.

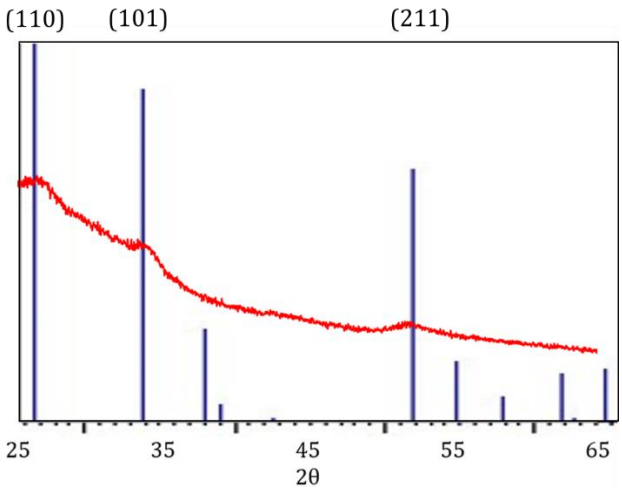

Figure 2.2.1.2. **X-Ray Diffraction (XRD) plot of Annealed SnO_2 films** Shown in red is the experimental XRD data. The published SnO_2 diffraction peaks are shown as blue lines. There is a clear correlation between the two, signifying the material sputtered in crystalline SnO_2.

2.2.2 Gold Nanolayer Deposition

After the SnO_2 film is annealed, the samples are once again loaded into the vacuum chamber where a thin layer of gold is deposited onto the surface. This thin layer is about 2nm, and while Au is a very expensive material each sample has less than a penny worth of gold on it.

The AuNPs are formed by annealing the thin film of gold at 400C for 2 hours. During the annealing process the gold film is dewetted to form gold nano islands that serve as AuNPs. The process of this NP formation is illustrated in Figure 2.2.2.1. These islands are 20 nm on average, this means that the AuNPS are absorbing light within the visible region, and this is based on simulated AuNPs that are 20nm in size. This data is seen in Figure 2.2.2.2, where the absorbance peak is at about 600nm which correlates to green light within the visible spectrum.

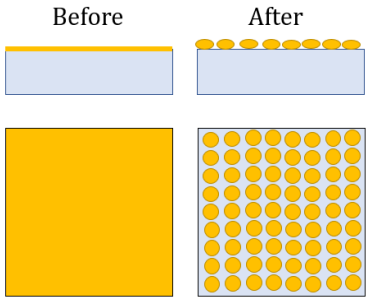

Figure 2.2.2.1. **Diagram of Gold Dewetting Process** In order to get AuNPs, a thin (2nm) layer of gold is first evaporated on to the samples, this leaves a flat film (as shown in 'Before'). The samples are then annealed at 400°C for 2 hours, at this temperature the gold restructures to nanoparticles on top of the surface (as shown in 'After').

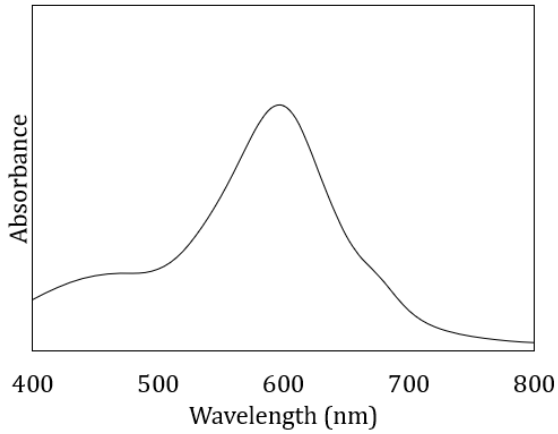

Figure 2.2.2.2. **Simulated Absorbance of 20nm Gold Nanoparticles** This data was simulated in JCM Wave. The simulated AuNPs exhibit an absorbance peak near 600nm. 20nm NPs are simulated because as the gold goes from a 2nm flat film to spheres, the estimated diameter of the spheres is ~20nm.

The aluminum backing now shows an increased absorbance over samples without an aluminum backing, Figure 2.2.2.3. This is beneficial to the system because as a photocatalytic system, absorbance of light energy is the important first step to catalyzing an ROS generation reaction.

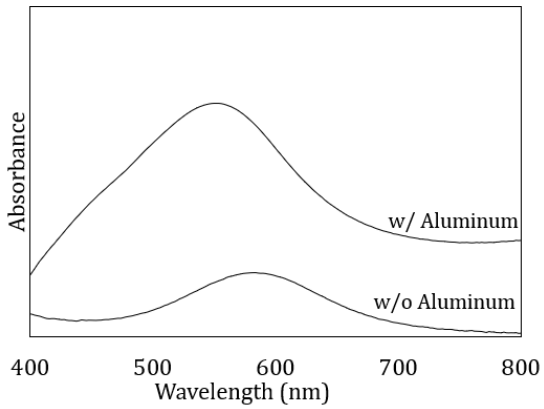

Figure 2.2.2.3. **Absorbance of Gold Nanoparticles in the Presence of an Aluminum Backing** Gold deposited via evaporation and then annealed to form nanoparticles has an absorbance peak within the visible light regime (~550nm, which translate to green light). The absorbance of this material can be intensified with an Aluminum backing. The peak exhibiting higher absorbance has a layer of aluminum behind the AuNPs.

2.2.3 Sample Characterization

Sample characterization is an important step other than absorbance within the visible light region, the duty of the AuNPs. It is also important that the SnO_2 is inactive in sunlight. This can be ensured through a band gap estimation using a Tauc Plot. The Tauc Plot is shown in Figure 2.2.3, and it estimates a band gap of 3.849, which correlates to 321nm light. This is a wavelength that is not useful due to the trivial amount provided in solar irradiance.

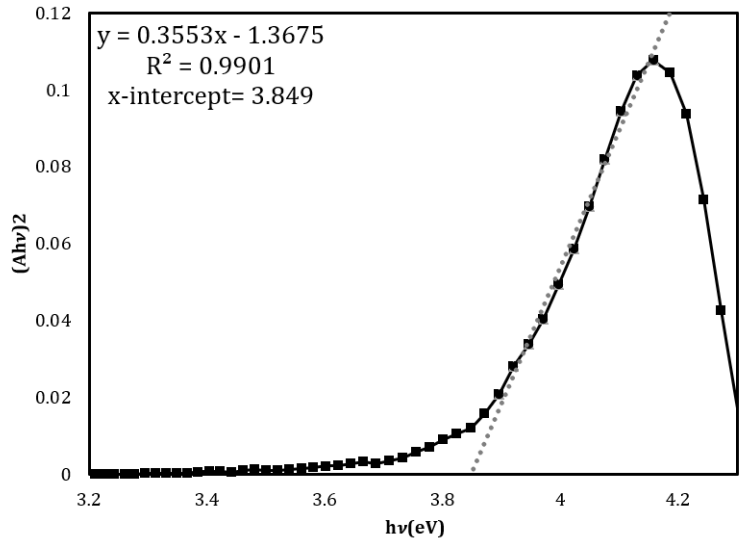

Figure 2.2.3. **Tauc Plot of Synthesized Films for Estimated Band Gap** Plotting energy in electron volts against the square of the product of experimental absorbance and each energy corresponding energy gives a graph with a steep downward slope, the x intercept of this slope is an estimate of the band gap. The estimated band gap of this SnO_2 film is 3.849

2.3 Results and Discussion

2.3.1 ROS Generation Testing Parameters and Methods

ROS is generated in many forms, as shown in Figure 1.2.2. However, in this research only one of these forms is tested for generation: H_2O_2. This is because it is a stable chemical that has a relatively long lifetime before degradation under the presence of only visible light.

The testing method for H_2O_2 is based on H_2O_2 concentration increase over time in a liquid that contains the sample. More specifically, the sample (Glass/Al/SnO_2/AuNPs) is placed at the bottom of a 50mL beaker. 25mL of water is then added to the beaker to cover the sample. This beaker is then placed on a shake plate for solar illumination. The shake plate constantly moves the sample to promote mass transfer of the H_2O_2 that has been generated. This general setup is modeled in Figure 2.3.1.1.

The solar illumination is done by a solar simulator. This is a machine that is made of many LED lights that mimic the concentration of each wavelength of sun with good precision to the sun's true irradiance. Figure 2.3.1.2 shows the spectrum of the solar simulator, both with and without a filter. The filter is a long pass filter than blocks any light over 455nm. This filter is chosen so that only visible light is reaching the sample (400-600nm), here 455 nm is being overcaution of blocking UV light.

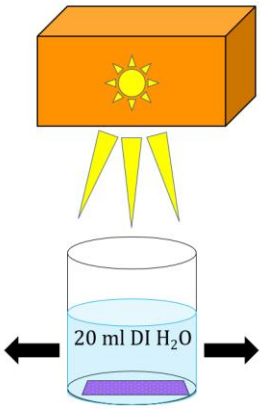

Figure 2.3.1.1. **Diagram of H_2O_2 Batch Generation Tests Using Solar Simulator** Samples are places at the bottom of a 50mL beaker and filler with 25mL of liquid. These beakers are shaken (to promote transfer) under the light of the solar simulator for time increments. ROS generation can then be determined form the liquid in the beakers.

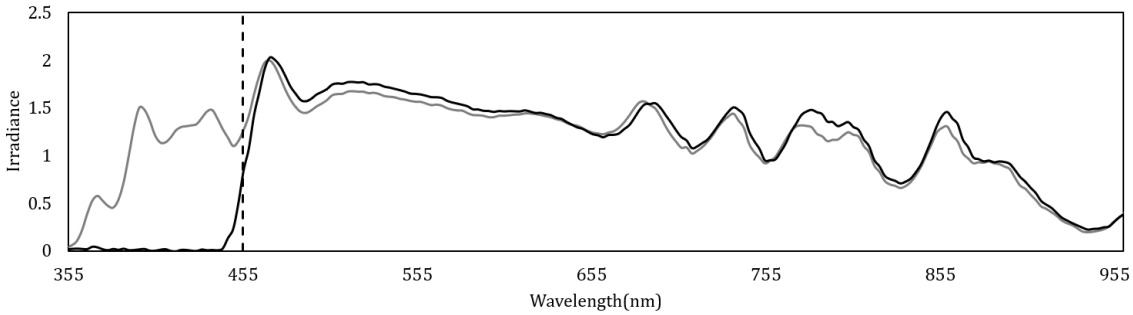

Figure 2.3.1.2. **Spectrum of Light from Solar Simulator** The program AM1.5 Simulates Solar Irradiance. The gray line indicates the spectrum of AM1.5G from the Wavelabs Solar Simulator. The Black line indicates the same AM1.5G irradiance with a below 455nm filter, used for sifting out UV and high energy visible light.

The samples are illuminated in the liquid that can be measured for H_2O_2 generation every 30-minute time interval. The H_2O_2 generation is measured using a fluorescent

probe. 2mL of the sample liquid and 1mL of RS+, a chemical that fluoresces under the presence H_2O_2 and is made of Amplex Red, Horseradish Peroxidase, and a buffer solution, this sample is then mixed and left to react for 2 minutes.

RS+ will fluoresce a bright pink color under the presence of H_2O_2, more brightly for higher concentrations. This fluorescence is measured using a fluorimeter. The sample is placed in a quartz cuvette and excited with a 520nm light. This method is illustrated in Figure 2.3.1.3. The sample then fluoresces and the emission at 590nm is measured. Each sample generates a fluorescence count curve over a short period of time, this fluorescence count is then averaged to give one count. A standard curve with known concentrations of H_2O_2 (0, 0.05, 0.1, 0.2, 0.5, 1, and 2 μM solutions) is generated using the same chemical and fluorescence method. The fluorescence count of each experimental sample can then be compared to this standard curve and the amount of H_2O_2 can be quantified.

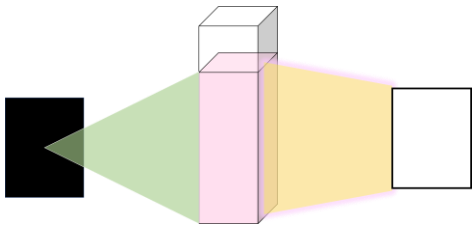

Figure 2.3.1.3. **Diagram of Fluorescence Tests Used to Determine ROS Generation** A fluorimeter shines light onto a cuvette holding liquid that the sample has generated ROS in and a chemical that fluoresces in the presence of H_2O_2 (the measured ROS species). The fluorescence of the sample is then measured and recorded.

2.3.2 Effect of Light on ROS Generation

Initial results are shown in Figure 2.3.2, and it can be concluded that ROS can be generated photo-catalytically using visible light. The wide band gap semiconductor without the presence of the AuNPs is inactive in sunlight with no $H2O_2$ generation, showing that the wide band gap semiconductor is used here only as an electron

acceptor and used as a reduction surface. The sample with AuNPs is illuminated under full sunlight (355+nm) and visible light only(455+nm). There is a very small difference these two which can conclude that visible light here is providing the power for the ROS generation in the solution.

While ROS is generated using visible light, it has extremely low efficiency, generating only 0.14μM of $H2O_2$. This can be due to low quantum efficiency, recombination, or most likely a combination of both. The effect of these two things is studied next.

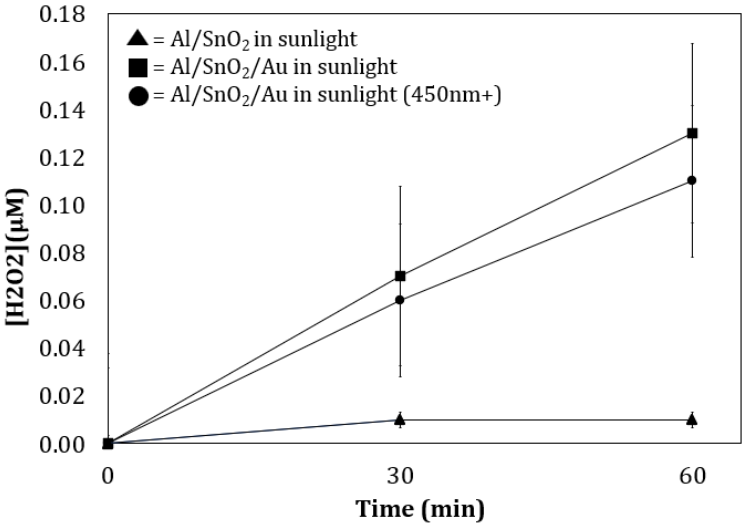

Figure 2.3.2. **H_2O_2 Generation of Tin Oxide and Gold Nanoparticle Samples in Various Light Conditions** The Al/SnO_2 samples without AuNPs (noted by triangles) shows minimal H_2O_2 generation under simulated sunlight. The Al/SnO_2/AuNPs samples in full sunlight exhibit the highest H_2O_2 generation. The Al/SnO_2/AuNPs samples in sunlight filtered to only be 450nm+ exhibit H_2O_2 generation similar to that of the samples in full sunlight, signifying that the light that is 450+nm is allowing for the majority of the H_2O_2 generation.

2.3.3 Effect of Hole Scavenger on ROS Generation

The effect of a hole scavenger on the H_2O_2 generation mechanism is meant to decrease incidences of hot electron/hole recombination. After an electron is excited out of the SP band in the AuNP, it is electronically favorable to recombine back into

that hole, leaving no work done. However, separation of these hot electrons from their holes is key to motivating an efficient system. Chemicals that easily give up electrons are called 'hole scavengers' because they remove the hole left behind by the excited electron and promote the electron to stay in its excited state until used. Ethanol is a cheap and widely used hole scavenger that is implemented in this research by using a 5% Ethanol in water solution as a H_2O_2 generation liquid rather than the previous DI water. Figure 2.3.3 shows results of the same samples tested in DI water and the Ethanol solution, and the sample generation over 30% more H_2O_2 in the ethanol solution. This effect can be connected to less recombination and more electrons successfully generation ROS. The H_2O_2 generation tests done are first tested in the dark for 30 minutes to ensure no H2O2 generation is for residual ROS, or non-visible light induced reactions.

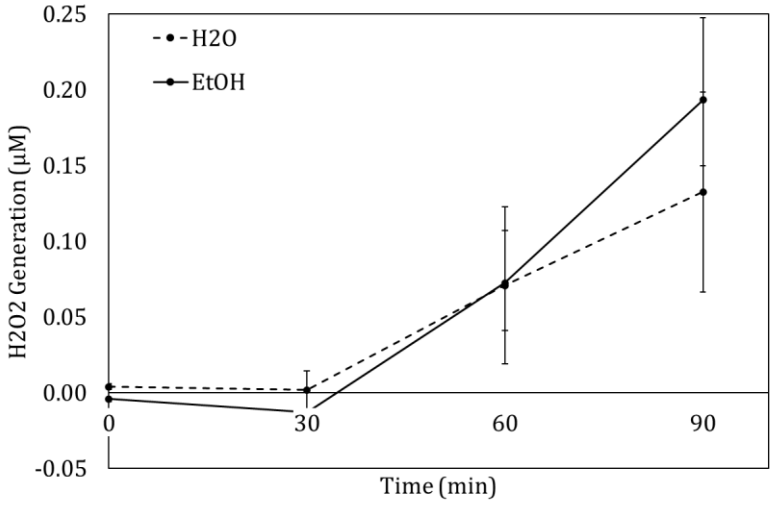

Figure 2.3.3. **Diagram of H_2O_2 Generation With and Without a Hole Scavenger Present** Samples illuminated for 60 minutes show increased H_2O_2 generation when in a 5% ethanol solution.

2.3.4 Effect of Oxygen Partial Pressure on ROS Generation

The effect of O_2 in the SnO_2 films is expected to change the electronic properties of the film and therefore the H_2O_2 generation capability. The Schottky barrier of the

SnO_2 films was measured using ultraviolet photoelectron spectroscopy (UPS), and it is possible that altering the O_2 concentration would change this. An illustration of this measurement is shown in Figure 2.3.4. In literature, it is shown that increasing the O_2 from 5% to 10% while sputtering increases crystallinity of the sample while maintaining the same band gap. However, while crystallinity is increased, the electron mobility is decreased. This would lead to less efficient H_2O_2 generation, as the mobility of electron being excited from the Au SP band would be limited. This being said, it is expected that increasing the O_2 concentration in the SnO_2 films would not improve the $H2O_2$ generation of the photocatalytic system.

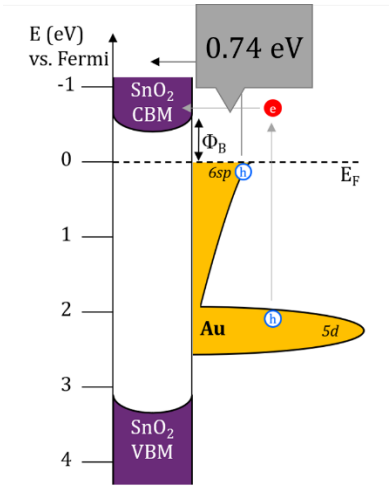

Figure 2.3.4.1. **Diagram of Band Positions of SnO_2-Au Schottky Junction** The Schottky Barrier was measured to be 0.74 eV using Ultraviolet Photoelectron Spectroscopy

Samples were made int eh same way as initially tested, SnO_2 films were sputtered in all the same conditions except the oxygen concentration in the working gas was changed to make samples with 5% O_2 and samples with 10% O_2. The gold nanoparticles were deposited the same way as initially stated. When tested using the same method for H_2O_2 generation, using a fluorescent probe and a fluorimeter, the samples with varying O_2 concentrations showed no statistical difference in H_2O_2

generation, this is shown in Figure 2.3.4.2. The same hold true with the samples are tested with the presence of a hole scavenger, or in a 5% ethanol solution, this is shown in Figure 2.3.4.3.

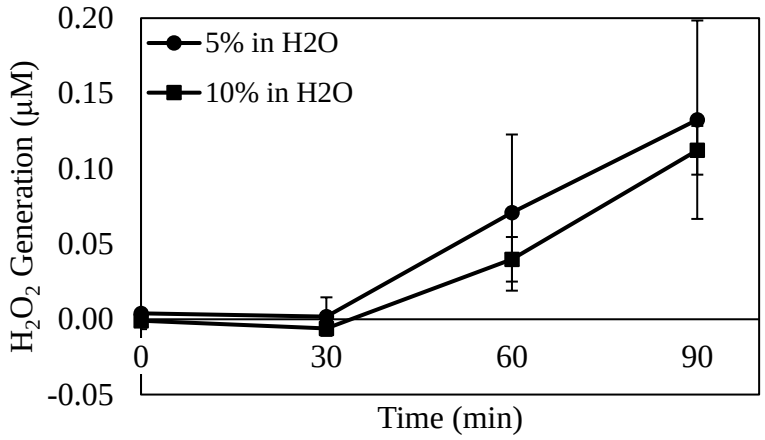

Figure 2.3.4.2. **H_2O_2 Generation of SnO_2/AuNPs Samples in Water with Varying Sputtering Oxygen Concentrations** Samples sputtered at 5 volume% and 10 volume% have no statistical difference in the amount of H_2O_2 they generate in DI H_2O.

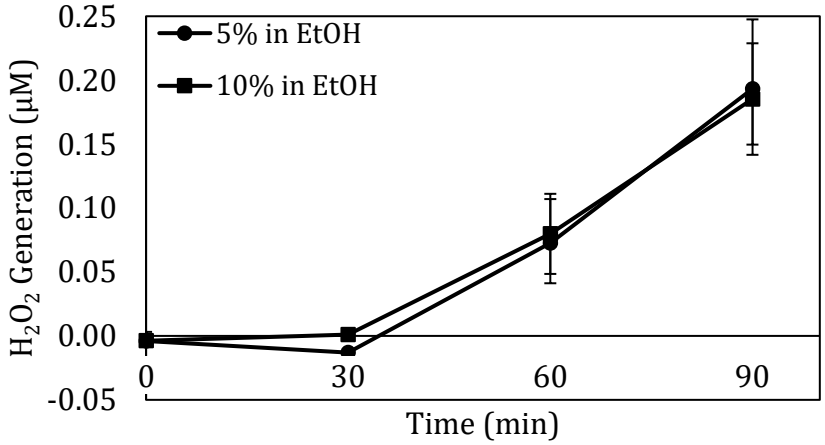

Figure 2.3.4.3. **H_2O_2 Generation of SnO_2/AuNPs Samples in 5% Ethanol Solution with Varying Sputtering Oxygen Concentrations** Samples sputtered at 5 volume% and 10 volume% have no statistical difference in the amount of H_2O_2 they generate in a 5% EtOH in water solution.

Chapter 3: Future Research ad Application

3.1 Structure Improvements

One of the major setbacks to $H2O_2$ production using this system is the limited contact area between the SnO_2 film and the AuNP. If the AuNP is a near spherical shape, and the semiconductor film is a flat surface, then the contact area is limited to wherever the AuNP surface was dewetted to. Embedding the AuNPs would greatly increase the area where the semiconductor and metal are in contact and promote much more electron transfer between the two, embedment of the NPs is illustrated in Figure 3.1. The limitation here is that the AuNP is the light absorber, so more light absorb leads to better $H2O_2$ generation efficiency, however there is an optimum balance of semiconductor/metal contact and metal nanoparticle light absorbance area.

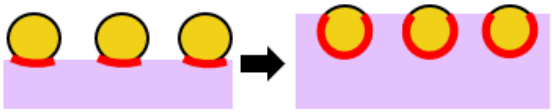

Figure 3.1. **Diagram of Gold Nanoparticles Embedded in a Tin Oxide Film**
Embedded AuNPs would have more contact surface with the Tin Oxide film, therefore a higher instance of electron transfer from the gold to the semiconductor.

3.2 Further Tests and Analysis

Other test that can be done to further study this system are generating an estimation of the band gap for the samples sputtered with 10% oxygen. This would allow confirmation of the hypothesis that changing oxygen concentration dos not change the bad gap. On the same token, XRD of the samples sputtered at 10% O_2 would confirm a higher crystallinity and in turn less mobility within the film. Sputtering the films at different powers has potential to change the band gap of the

films, so sputtering at powers other than 25W is a test that could prove to change H_2O_2 generation efficiency.

Lastly, future work may focus on a different application of this process. The current efficiency of this system leaves is virtually ineffective, but there are many alterations that could be made to improve this. Localized H_2O_2 generation is an issue that exists outside of water disinfection for the purpose of economic water scarcity. Other work focuses on localized H_2O_2 generation for the purpose of improving water reuse systems, and issue that will become important as drought is exacerbated by climate change. Overall, this system can make ROS using only the visible portion of sunlight, and this posed a great opportunity for cheap and easy ROS generation, however efficiency will have to be improved before further steps or application are taken.

Acknowledgements

It would be impossible to thank everybody who helped me get to the point where I am defending this thesis, however my first thank you goes out to Dr. Kevin McPeak. Dr. McPeak has been a gracious and patient mentor since I started my time at LSU in August of 2018. He has spent many hours teaching me theory, skills, and general scientific communication skills. He has also allowed me to take part in some opportunities at LSU I would otherwise not have been a part of. Working with Dr. McPeak inspired me to want to become a professor and continue a career in academia, specifically in water conservation.

I am also very grateful for the rest of the team that works and has worked in Dr. McPeak's lab. Although there are many projects and limited space, these people have been a sounding wall for ideas and great help throughout my years. Thank you to the graduate students: Daniel Willis, Luis Manuel, MaCayla Caso, Tiago Leite de Silva, Sara Stofela, and Mery Worbington. Thank you to the undergraduate students: Ella Sheets, Eryn Kennedy, Henry Kantrow, and Noah Smith.

Outside of my lab I would like to thank many of the professors in the Chemical Engineering Department for commitment to my education and thank you to the faculty working outside of the program who helped me obtain some of the results found within this paper. Thank you also to the LSU Ogden Honors College for the continued support and opportunity to present this and other projects many times. I would also like to thank LSU Discover for funding much of the research I was able to accomplish through the President's Future Leaders in Research Program.

I could thank everybody who has brought late night coffees and read abstracts and essays, but this thesis would become very long, so thank you to those who have supported me throughout my research career at LSU, I have only all of you to thank for the success I have had and the career I am pursuing, I am excited for what the future holds.

References

Badilescu, S.; Raju, D.; Bathini, S.; Packirisamy, M. Gold Nano-Island Platforms for Localized Surface Plasmon Resonance Sensing: A Short Review. Molecules 2020, 25, 4661. https://doi.org/10.3390/molecules25204661

Dan Leng, Lili Wu, Hongchao Jiang, Yu Zhao, Jingquan Zhang, Wei Li, Lianghuan Feng, "Preparation and Properties of SnO_2 Film Deposited by Magnetron Sputtering", International Journal of Photoenergy, vol. 2012, Article ID 235971, 6 pages, 2012. https://doi.org/10.1155/2012/235971

Daniel E. Willis, Mohammad M. Taheri, Orhan Kizilkaya, Tiago R. Leite, Laibao Zhang, Tochukwu Ofoegbuna, Kunlun Ding, James A. Dorman, Jason B. Baxter, and Kevin M. McPeak ACS Applied Materials & Interfaces 2020 12 (20), 22778-22788 DOI: 10.1021/acsami.0c00825

Fu, X., Li, G. G., Villarreal, E., & Wang, H. (2019). Hot carriers in action: multimodal photocatalysis on Au@SnO2 core–shell nanoparticles. Nanoscale, 11(15), 7324–7334. doi: 10.1039/c9nr02130b

Kisch, H. (2014). Semiconductor Photocatalysis. Semiconductor Photocatalysis. doi: 10.1002/9783527673315

Li, Y., Wen Zhang, W., Niu, J., Chen, Y. (2012). Mechanism of Photogenerated Reactive Oxygen Species and Correlation with the Antibacterial Properties of Engineered Metal-Oxide Nanoparticles. ACS Nano, 6(6), 5164-5173. DOI: 10.1021/nn300934k

Lorenzo, A., Area, S., Palella, A. (2018). Which Future Route in the Methanol Synthesis? Photocatalytic Reduction of CO_2, the New Challenge in the Solar Energy Exploitation. https://doi.org/10.1016/B978-0-444-63903-5.00016-9

McIntosh, Keith. (2011, June). The Extraterrestrial (AMO) Solar Spectrum. PVLighthouse. https://www2.pvlighthouse.com.au/resources/courses/altermatt/The%20Solar%20Spectrum/The%20extraterrestrial%20(AM0)%20solar%20spectrum.aspx

Pallavi Sharma et al, Journal of Botany, vol. 2012, Article ID 217037, 26 pages, 2012. doi:10.1155/2012/217037

Patrycja Makuła, Michał Pacia, and Wojciech Macyk. (2018). The Journal of Physical Chemistry Letters. 9 (23), 6814-6817. DOI: 10.1021/acs.jpclett.8b02892

Reference air mass 1.5 spectra. NREL.gov. (n.d.). Retrieved April 20, 2022, from https://www.nrel.gov/grid/solar-resource/spectra-am1.5.html

Selin Tosun, B., Feist, R., Gunawan, A. (2012). Sputter Deposition of Semicrystalline Tin Oxide Films. Thin Solid Films, Volume 520 (Issue 7), 2554-2561. https://doi.org/10.1016/j.tsf.2011.10.169

Serpone, N. (2000). Kirk-Othmer Encyclopedia of Chemical Technology. Photocatalysis. https://doi.org/10.1002/0471238961.1608152019051816.a01

Siahrostami, S., Li, G.-L., Viswanathan, V., & Nørskov, J. K. (2017). One- or Two-Electron Water Oxidation, Hydroxyl Radical, or H2O2 Evolution. The Journal of Physical Chemistry Letters, 8(6), 1157–1160. doi:

10.1021/acs.jpclett.6b02924Stofela, S. K., Kizilkaya, O., Diroll, B. T., Leite, T. R., Taheri, M. M., Willis, D. E., … McPeak, K. M. Noble-Transition Alloy Excels at Hot-Carrier Generation in the Near Infrared. Under Review.

Water treatment while hiking, camping, and traveling - cdc.gov. (n.d.). Retrieved April 20, 2022, from https://www.cdc.gov/healthywater/pdf/drinking/backcountry_water_treatment-508.pdf

United Nations. Scarcity, decade, Water For Life, 2015, UN-Water, United Nations,. United Nations. Retrieved April 20, 2022, from https://www.un.org/waterforlifedecade/scarcity.shtml

UV light. Stanford Solar Center. (n.d.). Retrieved April 20, 2022, from http://solar-center.stanford.edu/about/uvlight.html